ResearchGate

See discussions, stats, and author profiles for this publication at: https://www.researchgate.net/publication/215549300

Photodissociation of Formic Acid: A Trajectory Surface Hopping Study

ARTICLE *in* CHEMICAL PHYSICS LETTERS · AUGUST 2005

Impact Factor: 1.9 · DOI: 10.1016/j.cplett.2005.06.091

CITATIONS
13

READS
23

5 AUTHORS, INCLUDING:

Saulo A Vázquez
University of Santiago de Compostela
89 PUBLICATIONS **1,044** CITATIONS
SEE PROFILE

Giovanni Granucci
Università di Pisa
80 PUBLICATIONS **1,909** CITATIONS
SEE PROFILE

Maurizio Persico
Università di Pisa
153 PUBLICATIONS **6,219** CITATIONS
SEE PROFILE

Carlos Manuel Estévez Valcárcel
University of Santiago de Compostela
33 PUBLICATIONS **481** CITATIONS
SEE PROFILE

Available from: Emilio Martinez-Nuñez
Retrieved on: 23 January 2016

Available online at www.sciencedirect.com
SCIENCE DIRECT®
Chemical Physics Letters 412 (2005) 35–40
CHEMICAL PHYSICS LETTERS
www.elsevier.com/locate/cplett

Photodissociation of formic acid: A trajectory surface hopping study

Emilio Martínez-Núñez [a,b,*], Saulo Vázquez [a], Giovanni Granucci [b], Maurizio Persico [b], Carlos M. Estevez [c]

[a] Departamento de Química Física, Facultad de Química, Universidad de Santiago de Compostela, Avda das Ciencias s/n, Santiago de Compostela, E-15782, Spain
[b] Dipartimento di Chimica e Chimica Industriale, Università di Pisa, v. Risorgimento 35, I-56126 Pisa, Italy
[c] Departamento de Química Física, Universidad de Vigo, Vigo, E-3200, Spain

Received 27 May 2005
Available online 14 July 2005

Abstract

Non-adiabatic direct dynamics calculations were carried out to investigate the radical and molecular decomposition channels of formic acid. The calculations show, in agreement with experiment, that the HCO + OH dissociation channel accounts for ~70% of the product yields. In addition, the molecular eliminations of CO and CO_2 are minor channels, with a CO/CO_2 branching ratio that depends on what isomer is initially excited to the S_1 state. This result is also in qualitative agreement with experimental results in an Ar matrix environment.
© 2005 Elsevier B.V. All rights reserved.

1. Introduction

The photodissociation of formic acid (FA) has been well studied in the gas phase [1–18]. These are the radical and molecular channels that can occur in the photodissociation of FA (see Fig. 1)

$$FA \rightarrow HCO + OH \quad (1)$$
$$\rightarrow H + COOH \quad (2)$$
$$\rightarrow HCOO + H \quad (3)$$
$$\rightarrow H_2 + CO_2 \quad (4)$$
$$\rightarrow H_2O + CO \quad (5)$$

In a series of experimental papers it was suggested that the molecular elimination channels ((4) and (5)) proceed under dynamical control on the ground electronic state [15–17]. In other words, that the geometry of the transient species formed in the $S_1 \rightarrow S_0$ decay determines the product branching ratio. Photoexcitation of FA at 193 nm (~148 kcal/mol) in the gas phase also gives rise to CO and CO_2 after internal conversion (IC) to the ground state, but direct dissociation on the S_1 surface to give HCO + OH is the dominant channel. However, in an Ar matrix environment, Khriachtchev et al. [16] did not observe any isolated OH radicals, which suggests either a small cage-exit probability at this excitation energy (both radicals could rapidly recombine to FA) or a negligible branching ratio for this channel in solid Ar [16]. They found a CO/CO_2 ratio of ~0.4 for the photolysis of *cis*-FA, and ~5 for *trans*-FA. These results led them to propose a mechanism in the ground state (after IC) in which the elimination occurs faster than the randomization of the torsion coordinate mixing the conformers, thus following the previous suggestion by Su et al. [15]. However, our recent classical trajectory calculations are at odds with the idea of conformational memory in the ground state [18]. In particular our single state trajectory calculations predict almost identical CO/CO_2 branching ratios from the *cis* and *trans* conformers of FA and in very good accordance with RRKM calculations. In addition, when a specific vibrational

* Corresponding author. Fax: +34 981595012.
E-mail address: qfemilio@usc.es (E. Martínez-Núñez).

0009-2614/$ - see front matter © 2005 Elsevier B.V. All rights reserved.
doi:10.1016/j.cplett.2005.06.091

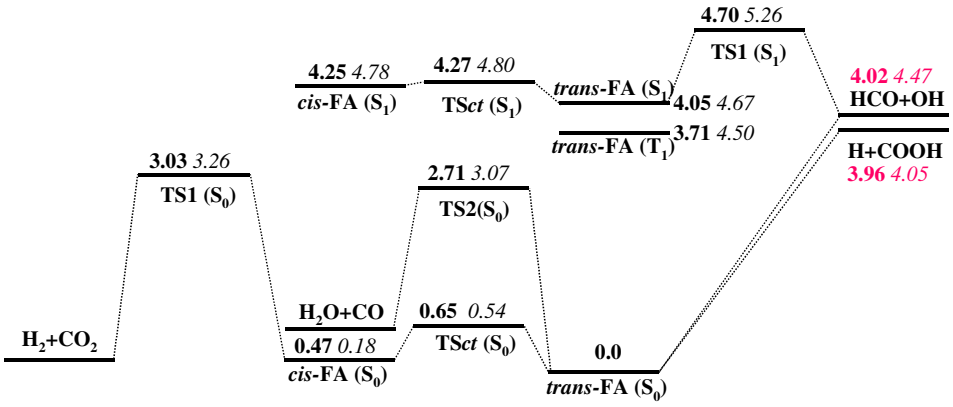

Fig. 1. Schematic potential energy diagram showing the channels considered in the present study. Bold figures are the AM1 results while italic figures correspond to ab initio calculations of [17,18]. Values in red correspond to chemical species not considered in the re-parametrization procedure.

excitation is used, to simulate more closely the internal conversion process, the branching ratio does not vary with respect to those obtained from the two conformers of the molecule. In our previous paper [18] we speculated on the causes for these differences between theory and the experiment of Khriachtchev et al. [16]. We indicated as possible sources of discrepancy the existence of additional internal conversion mechanisms that could trigger the $H_2 + CO_2$ process on the ground state. This possibility was corroborated by a geometry optimization on the S_0 state of an additional S_0/S_1 minimum crossing point (depicted in Fig. 2 as S_0/S_1 H_2), which leads to $H_2 + CO_2$. Another possible explanation for the different CO/CO_2 branching ratios could be the matrix environment and the possibility of strong cage effects. Actually, Khriachtchev et al. [16] did not find OH, while in previous studies in gas phase this was the major product at 193 nm. They explained their results [16] by stating

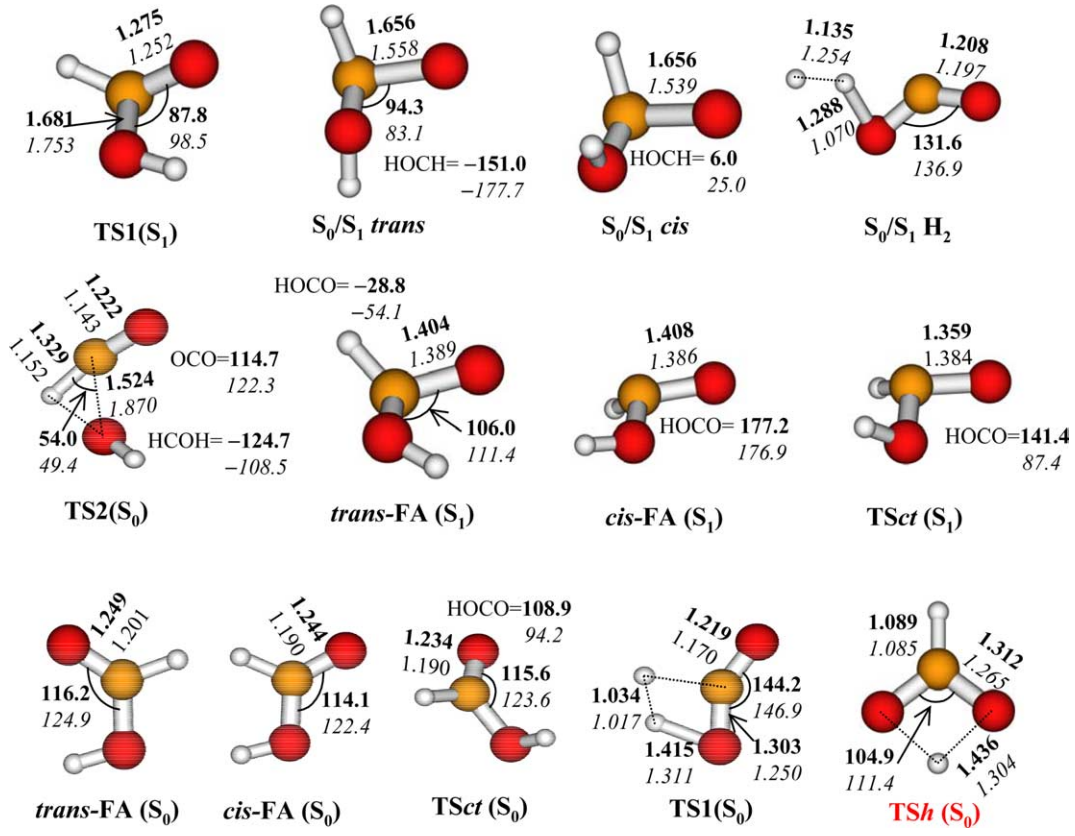

Fig. 2. Geometries of selected configurations in the S_0 and S_1 potential energy surfaces for formic acid used in the parametrization procedure. Bold figures are the AM1 results while italic figures correspond to ab initio calculations of [17,18]. Values in red correspond to chemical species not considered in the re-parametrization procedure.

that HCO + OH may recombine back to give FA again; i.e., cage effects would be very important in this system. In the present Letter we report trajectory surface hopping calculations for the study of the above mentioned dissociation channels of formic acid. The explicit treatment of the $S_1 \rightarrow S_0$ IC process will shed some light in the still obscure dissociation mechanisms of formic acid.

2. Methods

2.1. Semiempirical direct dynamics calculations

We employed the direct trajectory surface hopping method described in [19], based on semiempirical calculations of the electronic energies and wavefunctions, and on Tully's 'fewest switches' algorithm [20]. The AM1 Hamiltonian [21] was used for the electronic calculations. The molecular orbitals were obtained by the floating occupation SCF method [22], with the orbital energy width of 0.2 a.u. (5 doubly occupied orbitals and 8 with variable occupation numbers). With this orbital set a configuration interaction calculation of the CAS-CI type was performed with a complete active space of four electrons and four active orbitals. This wavefunction was found to be flexible enough to characterize the electronic states and dissociation pathways depicted in Fig. 1. These include dissociation channels (1), (2), (4) and (5). The radical channel giving rise to HCOO + H is higher in energy [17] and was not considered in the present study.

Additional ab initio calculations were carried out in the present study, in view of the necessary optimization of the semiempirical parameters. In particular, we employed the state averaged CASSCF/cc-pVTZ methodology with an active space comprising 10 electrons in 8 orbitals in order to explore the first singlet excited state potential energy surface. Only the ground and first excited singlet states were included in the state average calculation with equal weights. These calculations were performed with the GAUSSIAN-98 program [23]. We were able to find, not only the crossing points S_0/S_1 *cis* and S_0/S_1 *trans* reported previously by He et al. [17] but also a new crossing point S_0/S_1 H_2 located 1.29 eV above the S_1 global minimum (the *cis* and *trans* crossing points are 1.23 and 1.20 eV higher in energy than the S_1 minimum). To reproduce the present and previous ab initio calculations [17,18] the AM1 hamiltonian for carbon, oxygen and hydrogen was reparametrized by using the simplex method. The optimization process of the semiempirical parameter set has been described in detail elsewhere [24]. The energies of the stationary points depicted in Fig. 1 (in black) and their geometries (Fig. 2) were used as targets in the re-parametrization procedure, as well as the energies of S_0/S_1 *cis*, *trans* and H_2 crossing points (not shown in Fig. 1). The energies of these conical intersections, as calculated with our re-parametrized semiempirical Hamiltonian, are 1.26, 0.76 and 1.38 eV, respectively, which compare reasonably well with the CASSCF/cc-pVTZ calculations of the present work (see above). Table 1 shows the new parameter set. The main discrepancies for energies concern the energy difference between the global minimum of the S_1 and that of the S_0 surface (*trans* conformation in both cases): the energy gap is 4.05 eV at the AM1 level of theory while the MRCI value is 4.67 eV [17]. This difference of about 0.6 eV is essentially constant for all the stationary points on the S_1 surface. For geometries, major discrepancies occur for transition state TS2 as can be seen in Fig. 2. In addition, the carbonyl CO distances are consistently higher at the AM1 level of theory in comparison with the ab initio calculations. On the other hand, it was necessary to include the following analytical term to the electronic energies of both S_0 and S_1, in order to model accurately the stability of TS1:

$$U_{\text{add}} = D \cdot \text{SW}_1 \cdot \text{SW}_2,$$

where SW_1 and SW_2 are switching functions of the form

$$\text{SW}_i = 1/2\{1 + \tanh[g_i \cdot (h_i - r_i)]\}$$

with r_1 and r_2 being the H–H and C–H(2) distances, respectively. D was chosen to be 1.26 eV, $g_1 = g_2 = 8$ Å^{-1}, $h_1 = 1.3$ Å and $h_2 = 1.6$ Å. This analytical function lowers the value of the energy of TS1. The function only activates for geometries close to TS1 ($r_1 \sim 1$ Å and $r_2 \sim 1.2$ Å) and tends to zero otherwise; thus, it does not affect other regions of the potential energy surface.

Direct trajectory surface hopping calculations were carried out for the study of formic acid photodissociation dynamics, using the floating occupation SCF method [22] as implemented in a development version of the

Table 1
Optimized AM1 parameters used in our direct dynamics study

Parameter	Value
U_{ss}(C)	−52.485464
U_{pp}(C)	−37.122308
β_s(C)	−16.408444
β_p(C)	−7.736467
ξ_s(C)	1.827237
ξ_p(C)	1.661910
α(C)	2.625612
U_{ss}(O)	−101.964688
U_{pp}(O)	−78.108484
β_s(O)	−29.274369
β_p(O)	−29.465712
ξ_s(O)	3.046598
ξ_p(O)	2.546421
α(O)	4.410957
U_{ss}(H)	−10.259093
β_s(H)	−6.228635
ξ_s(H)	1.188007
α(H)	2.846274
G_{ss}(H)	12.865822

MOPAC package [25]. Non-adiabatic transition probabilities between electronic states were taken into account by means of the surface hopping method developed by Tully [20]. The trajectories were integrated with the velocity-Verlet algorithm using a step size of 0.05 fs, which results in an energy conservation of better than 0.007 % in 1 ps (<0.002 eV). Two batches of 106 trajectories were initiated from the *cis* or *trans* FA(S_0) isomers in their ground electronic and vibrational states. The cartesian coordinates and momenta were selected by using a Wigner distribution. Then a vertical excitation was performed by accepting those geometries with the S_0/S_1 energy difference in the range $E_v \pm \Delta E_v$, where $\Delta E_v = 0.1$ eV and $E_v = 5.8(5.6)$ eV. Ideally E_v should be 6.4 eV, which corresponds to a photon excitation of 193 nm, but unfortunately the above values were the best approximations we reached with our model calculations. Actually, we found no transitions in ensembles of 1000 trajectories for excitation energies of 6.0 eV or greater. To a large extent, this is because in our semiempirical potential the S_0–S_1 energy gap is 0.6 eV lower than that predicted by the high level MRCI calculations [17]. Additionally, since the 193 nm transition corresponds to an excitation of an electron from the nonbonding orbital on the oxygen atom to the antibonding $\pi^*(n \rightarrow \pi^*)$, and since the C=O distance increases by 0.189 Å (by MRCI calculations) while the AM1 increase in the C=O distance from S_0 to S_1 is only 0.156 Å, it is much more difficult to excite the molecule to high energies in our AM1 PES. From the 10^6 trajectories started from *cis* (*trans*) FA(S_0) only 4360 (3875) had the S_1 state energy lying in the above mentioned energy range.

3. Results and discussion

3.1. The radical channels

Table 2 collects the main results obtained in the present dynamics study. As can be seen in the table, for both *cis* and *trans* initializations, the radical HCO + OH channel is by far the major one: it accounts for 66–70% of the total number of reactive events. This result agrees very well with the experimental results of Singleton et al. [5–10] at 222 nm (~5.6 eV) of 70–80%. Additionally, we found that 49% (51%) of the OH production occurs on the S_0 state starting from the *cis* (*trans*) isomer, which is not surprising since the S_1 and S_0 states are degenerate at large $HCO(_2A')\ldots OH(2\Pi)$ distances. Actually, 94% (96%) of the HCO + OH products formed in the ground state funnel to S_0 after TS1(S_1) was already surmounted for the *cis* (*trans*) isomer. Up to 3% (2%) of the *cis* (*trans*) isomers undergo H migration between the oxygen atoms (on the ground state) leading to H(1)CO + OH(2) instead of H(2)CO + OH(1). The transition state responsible for such migration is depicted in Fig. 2 along with its main geometrical features [TS*h*(S_0)]. This transition state is predicted to be 1.83 eV above the *trans*-FA isomer in comparison with the CCSD(T)/aug-cc-pvtz value of 1.57 eV. It is remarkable that although this transition state was not used in the reparametrization procedure both its geometry and energy are well reproduced by our semiempirical calculations. To finish our analysis of the HCO + OH radical channel we note that 5% (10%) of these trajectories for *cis* (*trans*) dissociate directly on the S_1 state without any surface hopping. For the H + COOH channel we must say that up to 10% of the trajectories leading to these products experienced H migration between both O atoms through TS*h*(S_0), while 43% (26%) for *cis* (*trans*) trajectories funneled directly to the H + COOH products without redistributing the energy on the S_0 state.

Table 2
Branching ratios obtained in our direct dynamics study in comparison with experimental results

	DTSH[a]		Experiment	
	cis	*trans*	*cis*	*trans*
HCO + OH	66.29	69.96		70–80[b]
H + COOH	15.18	10.34		
CO + H_2O	17.13	18.85		
H_2 + CO_2	1.40	0.85		
CO/CO_2	12.2	22.3	0.42[c]	5[c]11[d]

[a] This work at 5.8 (5.6) eV.
[b] Singleton et al. [5–8,10] at 222 nm.
[c] Khriachtchev et al. [16] in solid Ar (at 193 nm).
[d] Su et al. [15] in gas phase at 193 nm.

3.2. The molecular channels

The most important result of our investigation is that we found a certain degree of specificity in our calculations, resembling the experimental results. The CO/CO_2 branching ratios calculated here for *cis* and *trans* isomers differ almost by a factor of two. This is in qualitative agreement with experiments carried out in Ar matrix, although in their case the branching ratios differ by a factor of 12 [16]. The trend also observed in our study is that when one initializes the trajectories from the *trans* isomer one gets more CO than starting from the *cis* isomer. Our results can be explained by the differences in the funneling geometries for *cis* and *trans* isomers. More than 30% of the H_2 + CO_2 reactive trajectories in the *cis* isomer funnel through geometries similar to those of S_0/S_1 H_2 in Fig. 2, and therefore the trajectories dissociate to the H_2 + CO_2 products right after the funneling process without time to redistribute the energy on the ground state. The remaining trajectories that give rise to H_2 + CO_2 funnel to the ground state trough S_0/S_1 *cis* or S_0/S_1 *trans* and redistribute the energy in the ground state. Since once the molecules redistribute

the energy on the ground state they lose the memory about the initial conditions, these trajectories will not make any difference between the *cis* and *trans* results for the CO/CO_2 branching ratios. Starting from the *trans* isomer, however, the percentage of trajectories (over the $H_2 + CO_2$ reactive events) funneling through S_0/S_1 H_2 is only 9% (ca. 3 times less than in the *cis* case), which explains the differences in the branching ratios. Fig. 3 shows three different mechanisms of $H_2 + CO_2$ production. In panel (a), the molecule funnels to S_0 and then isomerizes to *trans*-FA, which in turn isomerizes through TS*h*(S_0) to a *trans*′-FA isomer and then eliminates $H_2 + CO_2$. The trajectory in panel (b) is a typical trajectory that funnels to the ground state and after some redistribution of internal energy gives rise to H_2 through TS1(S_0). Finally, a typical trajectory funneling through the S_0/S_1 H_2 conical intersection is analyzed in detail in Fig. 3c. This trajectory suffers several surface hops: once it is in the ground state the CH bond is broken and the H atom goes in search of the other H atom, hops to the excited state and, in the end, funnels through the S_0/S_1 H_2 conical intersection.

To further study the influence of the S_0/S_1 H_2 conical intersection on the branching ratios we ran two additional batches of trajectories with a different re-parametrization of the AM1 Hamiltonian, in which we did not consider this geometry among the target data and employing again the analytical form detailed above.

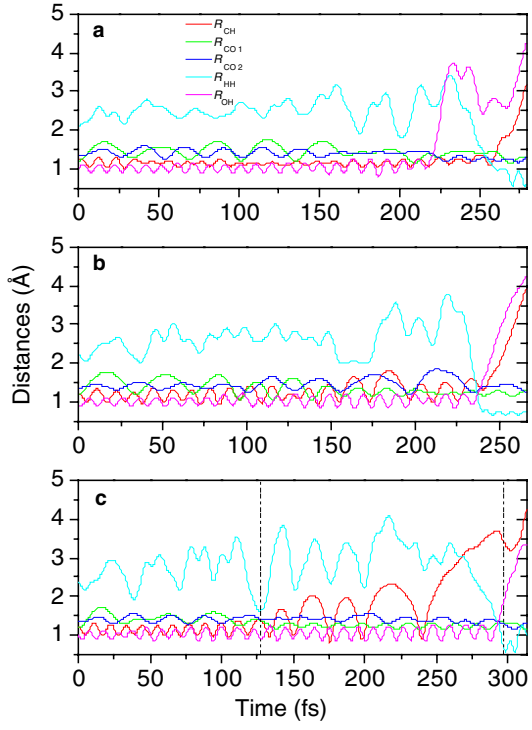

Fig. 3. Three typical trajectories for the $H_2 + CO_2$ channel. Vertical solid lines represent a $S_1 \rightarrow S_0$ surface crossing and vertical dashed lines represent $S_0 \rightarrow S_1$ surface crossings.

Actually with this new set of parameters we were not able to optimize the S_0/S_1 H_2 geometry corresponding to the minimum in a S_1/S_0 crossing seam. With this new parameter set our results resemble those obtained with the former one: the HCO + OH radical channel accounts for 57% (61%) of the reactive events, the H + COOH relative abundance is 20% (13%) for *cis* (*trans*), but the CO/CO_2 branching ratios are almost equal: 14 and 14.7 for *cis* and *trans*, respectively. These results corroborate the importance of the S_0/S_1 H_2 conical intersection in the production of $H_2 + CO_2$.

Although a certain degree of specificity has been brought out, our calculations do not reproduce quantitatively the experimental CO/CO_2 branching ratios obtained in [16]. Inaccuracies of the PES, including additional funneling mechanisms not found in our ab initio study, may be responsible for the observed discrepancies. In addition, cage effects may play a significant role in the dynamics. Particularly, H + COOH products might recombine to give $H_2 + CO_2$, which will result in a decrease of the CO/CO_2 branching ratios, specially for photoexcitation of *cis*-FA (see Table 2). However, only a dynamics study with an accurate potential energy surface including the environment (the Ar matrix) could tell us the story.

Finally, the percentage of trajectories that suffer H migration between the oxygen atoms in the $CO + H_2O$ channel is about 8% in both cases (*cis* and *trans*). The fact that the percentage of H migration is similar in both cases in another proof of out previous conclusion [18] that the photodissociation of formic acid does not present conformational memory on the ground state.

4. Conclusions

We carried out a direct dynamics surface hopping study of the photodissociation of formic acid. Our results agree qualitatively with experiment:

(1) The HCO + OH radical channel is the major one
(2) The CO/CO_2 branching ratio depends on the isomer initially excited.

The lack of quantitative agreement between our theoretical results and the experiment of Khriachtchev et al. [16] can be explained on the following grounds:

- Deficiencies in the potential energy surface, including the possibility of other funneling mechanisms not described by the present model.
- Strong cage effect in the Ar matrix. Since the H + COOH relative abundances are also different from the *cis* and *trans* isomers, this could help to improve the agreement between theory and experiment.

Acknowledgements

E.M.-N. thanks the Spanish Ministry of Science and Technology for his Ramón y Cajal research contract and Scuola di Dottorato Galileo Galilei for financial support during his stay in Pisa.

References

[1] H.C. Ramsperger, C.W. Porter, J. Am. Chem. Soc. 48 (1926) 1267.
[2] E. Gorin, H.S. Taylor, J. Am. Chem. Soc. 56 (1934) 2042.
[3] M. Burton, J. Am. Chem. Soc. 58 (1936) 1655.
[4] R. Gorden Jr., P. Ausloos, J. Phys. Chem. 65 (1961) 1033.
[5] G.S. Jolly, D.J. McKenney, D.L. Singleton, G. Paraskevopoulos, A.R. Bosard, J. Phys. Chem. 90 (1986) 6557.
[6] G.S. Jolly, D.L. Singleton, D.J. McKenney, G. Paraskevopoulos, J. Chem. Phys. 84 (1986) 6662.
[7] G.S. Jolly, D.L. Singleton, G. Paraskevopoulos, J. Phys. Chem. 91 (1987) 3463.
[8] D.L. Singleton, G. Paraskevopoulos, R.S. Irwin, G.S. Jolly, D.J. McKenney, J. Am. Chem. Soc. 110 (1988) 7786.
[9] M. Brouard, J. Omahony, Chem. Phys. Lett. 149 (1988) 45.
[10] D.L. Singleton, G. Paraskevopoulos, R.S. Irwin, J. Am. Chem. Soc. 111 (1989) 5248.
[11] T. Ebata, T. Amano, M. Ito, J. Chem. Phys. 90 (1989) 112.
[12] D.L. Singleton, G. Paraskevopoulos, R.S. Irwin, J. Phys. Chem. 94 (1990) 695.
[13] M. Brouard, J.P. Simons, J.X. Wang, Faraday Discuss. Chem. Soc. 91 (1991) 63.
[14] R.S. Irwin, D.L. Singleton, G. Paraskevopoulos, R. McLaren, Int. J. Chem. Kinet. 26 (1994) 219.
[15] H. Su, Y. He, F. Kong, W. Fang, R. Liu, J. Chem. Phys. 113 (2000) 1891.
[16] L. Khriachtchev, E. Maçôas, M. Pettersson, M. Räsänen, J. Am. Chem. Soc. 124 (2002) 10994.
[17] H.-Y. He, W.-H. Fang, J. Am. Chem. Soc. 125 (2003) 16139.
[18] E. Martínez-Núñez, S.A. Vázquez, I. Borges Jr., A.B. Rocha, C.M. Estévez, J.F. Castillo, F.J. Aoiz, J. Phys. Chem. A 109 (2005) 2836.
[19] G. Granucci, M. Persico, A. Toniolo, J. Chem. Phys. 114 (2001) 10608.
[20] J.C. Tully, J. Chem. Phys. 93 (1990) 1061.
[21] M.J.S. Dewar, E.G. Zoebisch, E.F. Healy, J.J.P. Stewart, J. Am. Chem. Soc. 107 (1985) 3902.
[22] G. Granucci, A. Toniolo, Chem. Phys. Lett. 325 (2000) 79.
[23] M.J. Frisch et al., Gaussian-98, Revision A.11, Gaussian Inc., Pittsburgh, PA, 1998.
[24] C. Ciminelli, G. Granucci, M. Persico, Chem. Eur. J. 10 (1994) 2327.
[25] J.J.P. Stewart, Mopac 2000, Fujitsu Limited, Tokio, Japan, 1999.